Indian Journal of Engineering & Materials Sciences
Vol. 27, February 2020, pp. 58-66

Effect of process parameters and VC content on structural and mechanical properties of WC-20Co nano composites

Devender Kumar[a] & Kulvir Singh[b]*

[a]Mechanical Engineering Department, Thapar Institute of Engineering and Technology Patiala, Punjab 147 004, India

[b]School of Physics and Materials Science, Thapar Institute of Engineering and Technology Patiala, Punjab 147 004, India

Received: 19 February 2019; Accepted: 22 August 2019

The effect of process parameters and vanadium carbide on hardness, toughness and structural properties of the tungsten carbide-cobalt (WC-Co) nanocomposite has been investigated using micro-hardness tester, X-ray diffraction and scanning electron microscopy (SEM) with attached energy dispersive spectroscopy, respectively. To suppress grain growth, a high percentage (upto 10 wt. %) of vanadium carbide (VC) has been taken as a grain growth inhibitor as well as a hardener. WC-20Co composite with 7.5 wt% VC, heat treated at 1100 °C holding time for 2 hours, possesses high hardness (1687 HV) when the volume fraction of tungsten carbide (WC) and Co_6W_6C phases have been taken in the ratio of 2:1. High hardness and toughness have been obtained at 1100 °C for 2 h heat-treated sample. High VC content with 8 h holding time has increased the porosity in the samples.

Keywords: Tungsten-carbide, Nanocomposites, High-hardness, Fracture toughness

1 Introduction

Mechanical properties of nanocomposites are very sensitive to the density, microstructure, and presence of various crystalline phases with their volume fractions. Processing parameters and initial constituents of the mixture are prime contributors for controlling these properties[1,2]. Densification of sintered ceramic material is always an arduous task[3]. Proper selection of binder material not only helps to improve mechanical properties, but also increases sinterability of the tungsten carbide[4,5]. Similarly, doping by VC, Cr_3C_2, TaC, TiC, NbC or CeO_2, act as grain growth inhibitors to improve hardness without much compromise in physical properties of WC-Co composite[6-10].

WC exhibits high hardness and offers superior protection against wear and abrasion of the tool surface. However, its poor ductility restricts its application, as a tool and dies material. WC-Co composites as tool materials need high hardness and reasonably good toughness to sustain thermal shocks and variable cutting parameters. WC-Co is widely used as a low cost, highly durable, chip-less bulk material for cutting tools. Modern thin-film coated tools are prevalent for special purpose machining operations. Despite several superior abilities of coated tools, like high operating temperature, high cutting speed, longer tool life etc., they are not generally accepted due to very high initial cost, chip-off defects and non-repair ability in case of minute damage. Development of WC-Co nanocomposites would be very good substitute to the coated tools.

Mechanical properties of any composite depend on the interface formed between matrix materials and the particulates[3,6,11-13]. Amongst various metal binders, Co is widely used as a matrix material due to its excellent wettability with hard WC as the particulates. Much work has been reported on the synthesis and characteristics of WC-Co nanoceramics with the variable cobalt content and particle sizes[6,14-18].

Restricting grain growth and achieving high densification is a big challenge in most of the ceramic materials. Fine-grained WC-Co nanocomposites possess superior mechanical and structural properties compared to coarse-grained composites. It is commonly reported that initial powder particle size, sintering temperature and its duration exhibit very strong correlation for obtaining superior mechanical properties[3,16,19-26]. Grains grow abruptly while sintering nano/micro sized WC-Co powders at1100-1400 °C[1,7]. Whereas, initial heating up to 1100°C and holding at 1400 °C showed very little grain growth. There are correlations between the densification behaviors of WC-Co composites using a low

*Corresponding author (E-mail: kusingh@thapar.edu)

percentage of VC, for controlling grain size[19,27-35]. Role of VC as a grain growth inhibitor is more noticeable in conventional liquid phase sintering compared to other fast sintering techniques[36]. VC can also act as a hardener for increasing hardness, wear resistance and densification of WC-Co composites[9,37].

Use of nano WC powder as raw material helps to produce high hardness nanocomposites with good densification[15-38]. Fang *et al.*[14] found 30% increase in toughness of WC-Co nanocomposites using nanopowderas compared to coarse powder, although there is less evidence supporting the coexistence of high hardness with high toughness[37,39,40]. Furthermore, there are some reports on the effect of high wt. % vanadium carbide as a grain growth inhibitor with high cobalt content[21,40]. In the present study, it is expected that nanocrystalline WC powder would result in good inter diffusion and inter-deformation among various initial components of the samples. On the other hand, high cobalt content tends to increase the dissolution of WC and C, whereas more VC suppresses grain growth during long holding times[1,11]. Additionally, the role of VC as hardening agent is also evident [7,35]. Deficiency of carbon, leads to the formation of Co_6W_6C phase and agglomeration of Co and VC over long holding time. This study is related to the effect of process parameters and vanadium carbide content on evolution of different crystalline phases. The effect of these evaluated crystalline phases on structural and mechanical properties is reported for WC- 20Co along with variable wt. % VC and process parameters.

2 Materials and Methods

2.1 Preparation of samples

The samples heat treated at 1100 °C with different holding time are given in Table 1. All the samples were prepared by solid-state reaction method in commercial argon atmosphere. The purity of all the chemicals was ≥ 99.9%. The tungsten carbide nanopowder (55 nm) and vanadium carbide nanopowder (600 nm) were procured from US Research Nanomaterials, USA and cobalt powder was procured from Sigma Aldrich, USA. The powders were mixed for 2 h in wet media, having 20 wt. % Co and variable wt. % (2.5, 5, 7.5 and 10) of vanadium carbide. The mixed powder was dried at 110 °C in a vacuum oven for 1 h. The dried mixture was ground again for few minutes in an agate mortar and pestle to break any agglomerates developed during drying process. A specially designed tungsten carbide die-set[41] was used to uni-axially compress at 15 Tons (1.875 kN/mm^2) to made the pellets of10 mm diameter and 1.6 mm thickness, using a hydraulic press (Polyhedron, India- Model 5010). The pressure was more than the pressure used by few other researchers for achieving better diffusion among initial constituents during sintering[2,42-47]. The pellets were sintered at 1100 °C with heating rate of 5 °C and holding for 2, 4, 6 and 8 h in a commercial argon atmosphere.

2.2 Characterization and testing

The relative densities of the sintered pellets were calculated using Archimedes principle at room temperature. X-ray diffraction patterns between $25° < 2\theta < 80°$ (scanning speed 5° per min.) of the sintered samples were analyzed with PANalytical Xpert-Pro using radiations of CuK_α (λ = 1.54 Å) with an inbuilt nickel filter. The volume fractions of the different crystalline phases formed during sintering were calculated by direct comparison method[48] using the XRD diffraction data. After sintering, all the samples were fractured and coated using JEOL's sputtering machine for scanning electron microscopy (SEM) studies. Energy dispersive spectroscopy (EDS) was performed using JEOL-JSM-6510, Japan. Diametrically sectioned (Fig. 1) samples were polished for making indentations. Vickers hardness was measured using Mitutoyo (MVK-HO, Japan) micro-hardness tester. Average values of hardness were calculated from five indentations across the length and thickness of the cross section of the pellet. Fracture toughness of the

Table 1 — Samples of WC-20 wt% Co-VC with variable holding time at 1100 °C.

Sample No.	VC wt. %	Isothermal Holding (h)
P2	2.5	2
P3	5.0	2
P4	7.5	2
P5	10.0	2
P6	2.5	4
P7	5.0	4
P8	7.5	4
P9	10.0	4
P10	2.5	6
P11	5.0	6
P12	7.5	6
P13	10.0	6
P14	2.5	8
P15	5.0	8
P16	7.5	8
P17	10.0	8

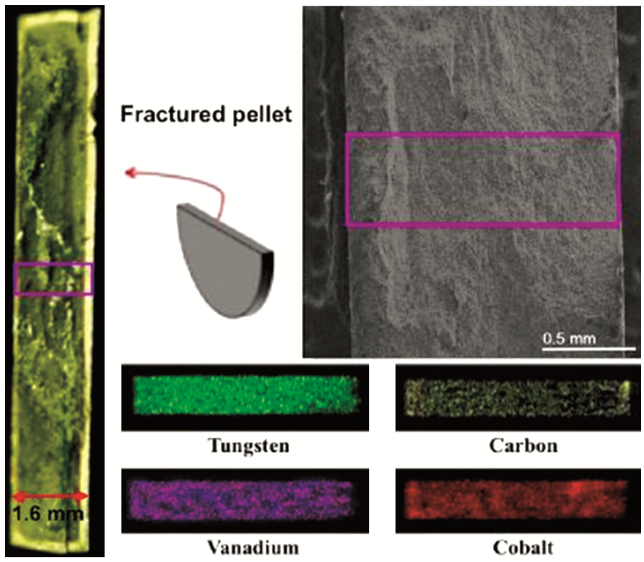

Fig. 1 — Distribution of different elements tested by X-ray dot mapping of P2 sample heat treated at 1100 °C for 2 h holding time.

sintered pellets were measured using Vickers indentation and equation (1) based on median crack system and gives indentation fracture toughness (IFT)[43,49,50] under 10 kg indentation load.

$$K_{IC} = 0.016(P)\,(E/H)^{1/2}(C)^{-3/2} \quad \ldots (1)$$

where P= load (kg), E= Young's modulus (GPa), H= hardness (kgf/mm^2) and C= crack length (mm), K_{IC} = fracture toughness (MN/m$^{3/2}$).

To obtain average values of hardness and fracture toughness, three different locations for indentations were considered for each sample. Crack length was measured with Nikon 3300 Metallurgical Microscope at different resolutions.

3 Results and Discussion

3.1 Density

The schematic of pellet sectioning and X-ray dot mapping micrographs of sectioned sintered pellet of P2 sample holding for 2 h is shown in Fig. 1. The distribution of W, C, V and Co throughout the pellet was uniform. Densities of the sintered samples and its variation with holding time are presented in Fig. 2, and density increased with increasing sintering time[1,3,8,14]. There was appreciable increase in densities of the samples containing 2.5 to 10 wt. % of VC upto 4 h of sintering time. Nevertheless, as sintering time was further increased, all samples show a decreasing trend in density, except for the samples having only 2.5 wt. % VC. Sample with 8 h sintering time shows

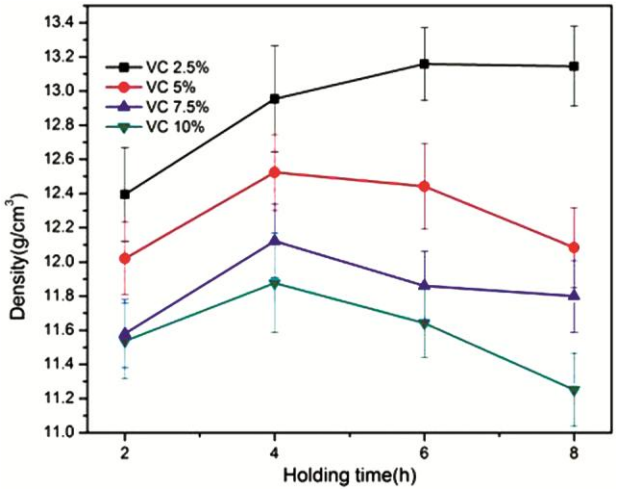

Fig. 2 — Density of the sintered samples for different holding duration.

poor density due to highly porous outer layer of the sample. It might be associated with the higher CO_2 formation, since some oxygen might present in commercial argon leads to react with pellets usually decompose at 350 °C and liberates carbon[11]. Sintering was carried out in a commercial argon atmosphere, even high surface area of nanopowders may act as carrier of oxygen during preprocessing of powder. Among all the samples, the continuous increasing trend of density with increase in sintering time was only followed by the samples containing 2.5 wt. % VC. From Fig. 2, it was found that very high percentage of VC did not play any significant role in densification; however the effect of VC as a hardening agent can be observed in samples with 7.5 wt. % VC[45,51-53] with holding time of two hours. In addition of VC in WC-20% Co would decrease the overall density of the sample. Since, the density of VC (5.77g/cc) is lesser than the density of WC (15.63 g/cc) and Co (8.90 g/cc). Additionally, formation of V_6C_5 and its segregation along grain boundaries act as grain inhibitor (discussed in section 3.4) lead to decrease the grain size and increase the grain boundaries. Thus, it decreases the density of the samples. It is well reported in the literature that VC, $Cr_2O_3$and processing parameters play very important role in densification and mechanical properties of tungsten carbide[10,54-56].

3.2 XRD analysis

The X-ray diffraction patterns of the sintered pellets are shown in Fig. 3 along with various crystalline phases formed during sintering. These

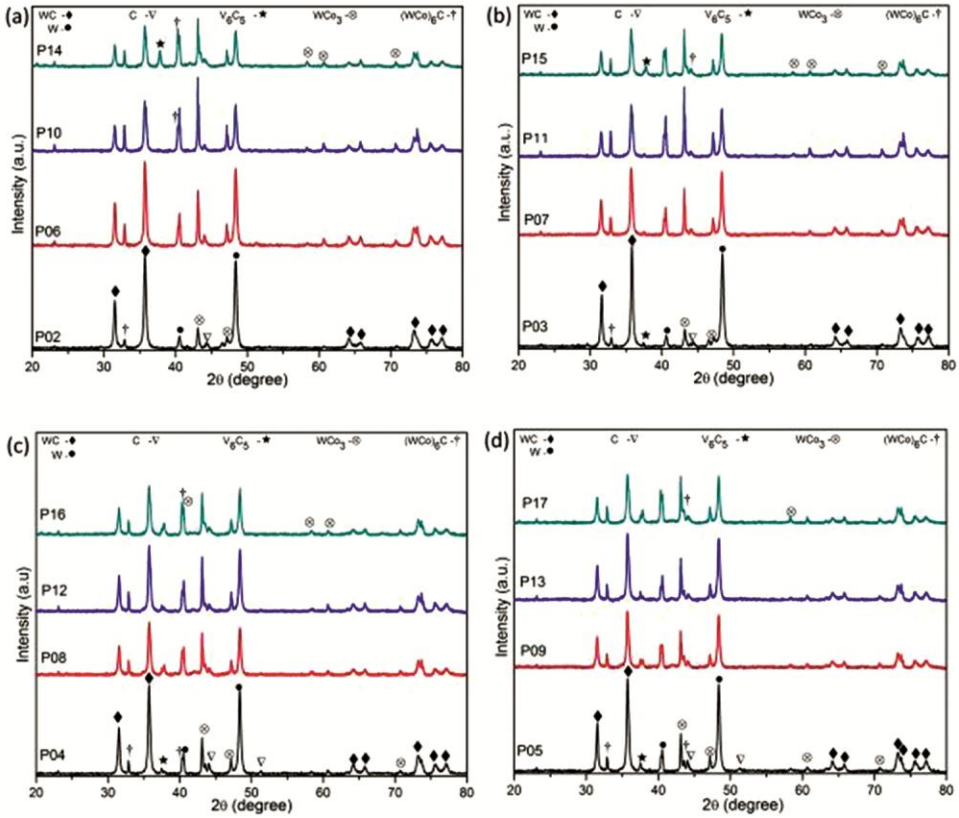

Fig. 3 — X-ray diffraction patterns of the samples (a) P2, P6, P10, P14, (b) P3, P7, P11, P15, (c) P4, P8, P12, P16 and (d) P5, P9, P13 and P17.

crystalline phases were indexed with different ICDD files: ICDD 00-023-0939, ICDD 01-089-2727, ICDD 01-080-2287, ICDD 01-080-0027 and ICDD 01-089-2767. The most common crystalline phases in appreciable volume fractions were Co_6W_6C (η phase), WC, V_6C_5 and W. The formation and volume fraction of W, WC, and W_2C depends on process parameters[57]. However, their volume fraction changed with sintering time and VC wt. % as given in Table 2. Additionally, some new phases with very small volume were also formed. It seems that WC initially decomposes and liberated some carbon. At the same time, there was diffusion of Co in the carbon depleted WC, which formed Co_6W_6C phase. It is also reported in the literature that formation of Co_6W_6C phase start at 1100 °C and increases with increase in sintering temperature[4,11,16]. The volume fraction of η phase was highly dependent on sintering time and VC content. As shown in Fig. 4, rise in isothermal holding time up to 6 h and 7.5 wt % VC, increased the volume fraction of Co_6W_6C at the cost of WC. Further, holding time increases up to 8 h, volume fraction of Co_6W_6C phase decreases as given in Table 2. Decomposition of VC generally starts above 350 °C[11], whereas WC is stable up to 700 °C[49]. The qualitative calculations for the volume fraction of different crystalline phases clearly suggest that the decomposition was mostly taken place from VC, instead of WC. The appreciable amount of η phase was formed in all the samples. The free carbon did not show any observable trend with increasing sintering time. However, after 6 h of heat treatment, the volume fraction of major phases, found to be reduced in all the samples. Interestingly, 8 h of holding time decomposed WC into W and CO_2.Increase in isothermal hold time gives a clear pattern for the formation of Co_6W_6C, V_6C_5 and W. Even so, phases like $VC_{0.75}$, C and W_2C does not follow any definite pattern with respect to sintering time and initial wt. % of VC (Fig. 4). The mechanism of different crystalline phase formation can be explained on the basis of following reaction:

$$14WC + 6VC + 6Co + 5O_2 \rightarrow Co_6W_6C + V_6C_5 + 8W + 9C + 5CO_2 \quad \ldots (2)$$

$$Co_6W_6C + 5C \rightarrow 6WC + Co \quad \ldots (3)$$

Table 2 — Volume fraction of different phases formed after sintering WC-20 Co-VC at 1100 °C.

Holding time	Vol. Fraction (%)	VC=2.5 %	VC=5.0 %	VC=7.5 %	VC=10 %
		P 2	P 3	P 4	P 5
	Co_6W_6C	17.33	12.43	28.7	28.39
	WC	76.58	83.17	61.39	59.63
	V_6C_5	--	--	4.09	5.63
2 hrs	C	4.36	1.79	5.79	6.34
	VC	1.21	--	--	--
	Co_3W	0.47	2.6	--	--
	V_2C	--	--	--	--
		P 6	P 7	P 8	P 9
	Co_6W_6C	37.14	41.37	40	35.6
	WC	47.04	49.31	45.16	48.22
	V_6C_5	10.06	2.17	8.68	6.49
4 hrs	C	5.75	3.08	4.11	3.75
	VC	--	--	0.4	$VC_{0.75}$=5.93
	Co_3W	--	4.05	W_2C= 0.8	--
	V_2C	--	--	0.8	--
		P 10	P 11	P 12	P 13
	Co_6W_6C	45.63	54.46	42.78	34.89
	WC	31	40.96	45.17	53.05
	V_6C_5	19.75	3.27	4.68	7.34
6 hrs	C	3.57	1.28	4.8	4.69
	VC	--	--	$VC_{0.75}$=2.4	--
	Co_3W	--	--	--	--
	V_2C	--	--	--	--
		P 14	P 15	P 16	P 17
	Co_6W_6C	34.62	35.2	29.4	30.87
	WC	28.55	34.66	31.16	32.12
	V_6C_5	10.89	6.4	4.2	4.63
8 hrs	C	--	5.3	4.6	4.15
	VC	--	--	$VC_{0.75}$= 8.25	2.92
	Co_3W	--	0.4	--	4.73
	V_2C	--	--	--	--
	W	25.93	17.8	22.33	20.55

3.3 Microstructure of WC-20Co composite

SEM micrographs (Fig. 5) clearly showed the increased porosity with the increase in VC at higher holding time. Microstructure of sample P4 sintered for 2 h (Fig. 5 (a)) indicated that particles were relatively denser in sample P4 as compared to P5, P12 and P15 (Fig. 5 (b), (c), (d)), which were sintered for longer holding time. Already published literature also raised the concern of grain growth during longer holding time[1-8,11,14,35,56]. Detailed investigation found that grain can growth from 49 nm to 640 nm during 400 min. of holding time. Few reports describe the grain growth phenomenon with coalescence of nanoparticles[1-3]. The network-like structure formed due to agglomeration and partial melting can be easily seen in Fig. 5(b), (c) and (d) when holding time was increased to 8 h at 1100 °C, whereas the similar effect with comparable morphology was reported by many other researchers at a much higher temperature[1-3,6,16,21]. In general, use of smaller particles facilitates more energy per unit volume and more surface area which decreases the sintering time and temperature [26]. Choosing low sintering temperature for nanoparticles along with high wt. % of VC for long holding times reflects increase in hardness and complete sintering in two samples. All samples were not completely sintered at low temperature by using nanopowder[6]. At lower sintering temperature, the viscosity of the binder is high enough which could not flow and fill the nano pores between

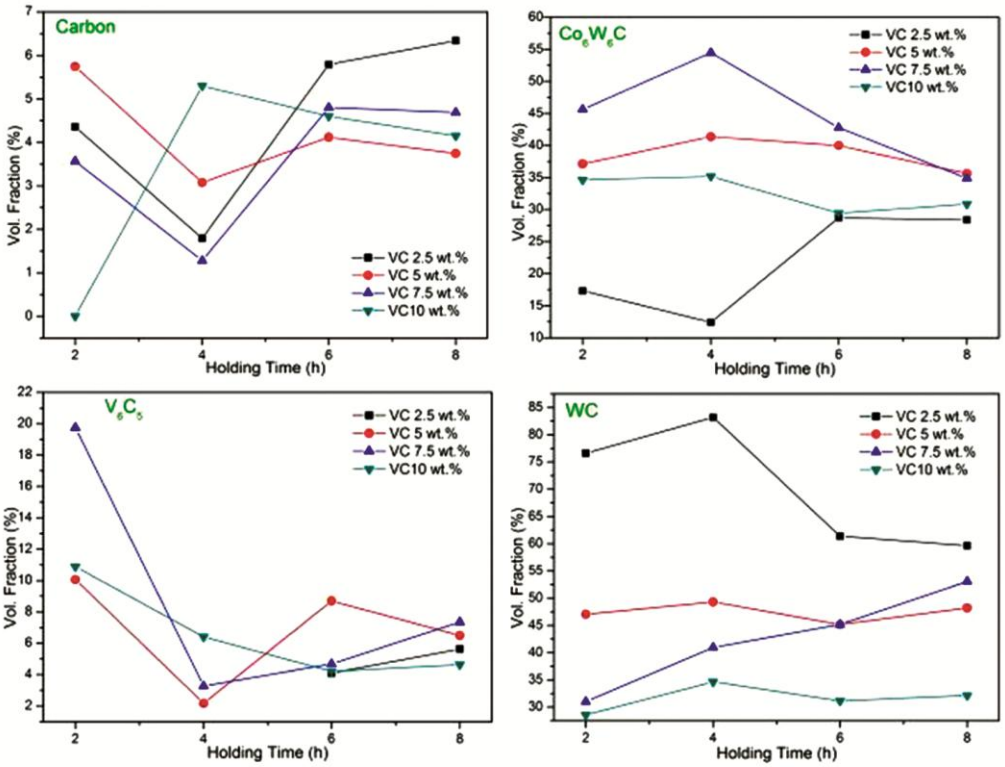

Fig. 4 — Volume fraction of crystalline phases (a) C, (b) Co_6W_6C ,(c) V_6C_5 and (d) WC.

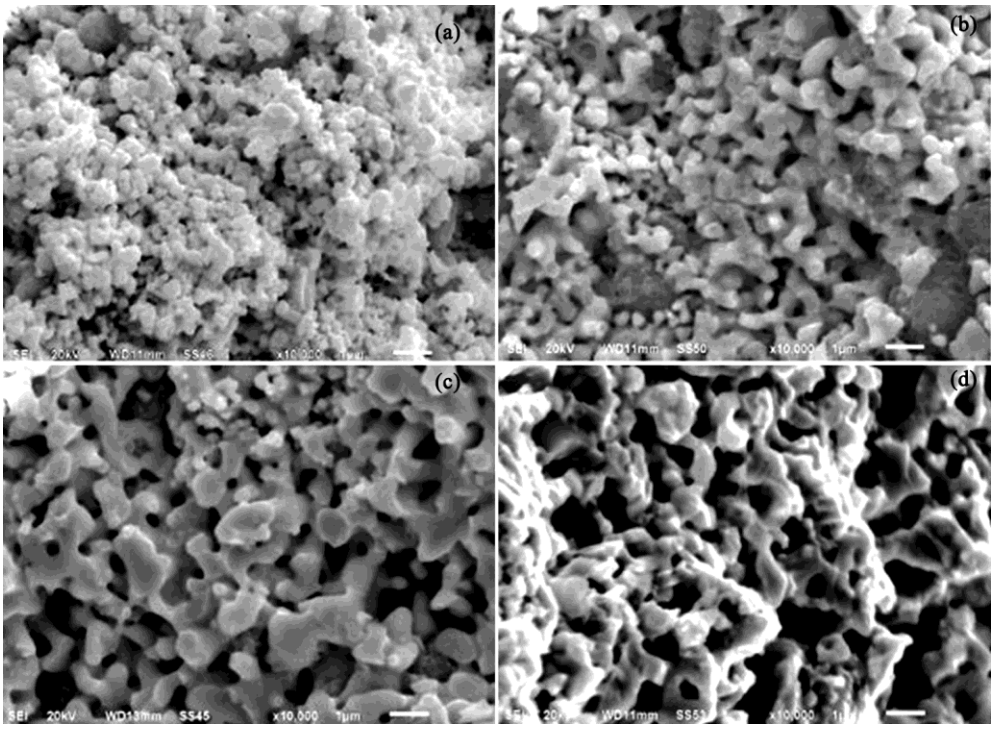

Fig. 5 — SEM micrographs of (a) WC-20 Co-7.5 VC sintered for 2 h, (b) WC-20Co-10 VC sintered at for 2 h (c) WC-20 Co-7.5 VC sintered for 6 h and (d) WC-20Co-10VC sintered for 8 h.

nano sized WC. It reduces the contact among particles during sintering at lower temperature. In sample P12, long sintering time leads to developed porous microstructure in the outer layer of the samples as shown in Fig. 5(c). There was no neck formation among the particles of samples, which were sintered for smaller duration (Fig. 5(a)). Small initial particle size of WC and high cobalt content helps to improve microstructure of WC-Co composite when sintered for small sintering duration[1-3,6,28].

In addition to this, further micro structural analysis was carried out on sample P14 to check agglomeration of VC, W or Co and the effects of long holding time. It was observed from the high-resolution images (Fig. 6) of the fractured pellets that there was formation of thick layer on the outer periphery of the sintered pellet. The layer was mainly composed of η phase, which becomes thicker with the increase in time. As shown in Fig. 7, three different regions were developed within the sample P14, sintered for 8 h. Region 1 was the outer shell having porous structure formed due to deficiency of carbon (liberated from WC and VC) and agglomeration of vanadium. SEM and EDS analysis (Fig. 7) confirmed the presence of small agglomerates of size 5-10μm and comprised 28 wt. % of O, 50wt. % of V and 18 wt. % of C. Region 2 consisted of relatively dense structure, having WC as the major phase without large agglomerates of VC. Apart from agglomerates of vanadium, region 3 was similar to region 2. Migration of cobalt in the liquid phase within region 3 during long sintering may lead to form agglomerates of vanadium. Agglomeration of binder phase and VC leads to bring WC particles in contact with each other.

The development of these regions was not equal in all the samples. It was observed that growth of brittle outer layer (η phase) was independent of the amount

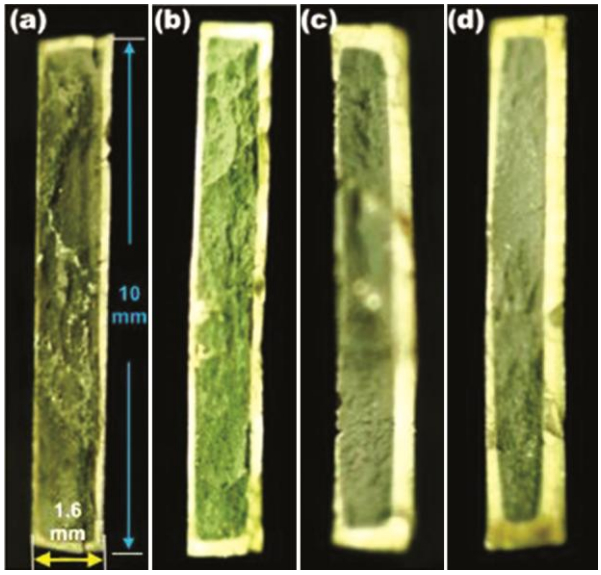

Fig. 6 — Brittle Eta-phase (Co_6W_6)C at the outer layer for different holding time (a) P2 for 2 h, (b) P6 for 4 h, (c) P10 for 6 h and (d) P14 for 8 h.

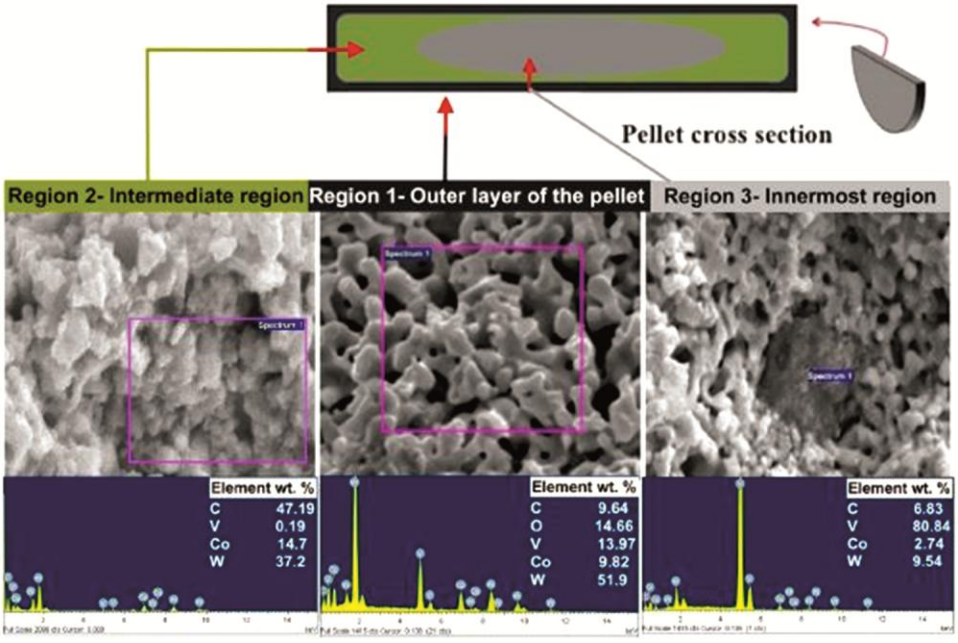

Fig. 7 — Microstructure and EDS of sample P14 with 8 h holding time (region 1) at the outer periphery with network like structure of eta phase, (region 2) agglomerates of cobalt, (region 3) agglomerates of vanadium.

of VC and increased with increase in holding time. Probably, as holding time was increased, the diffusion of smaller cations[50] like W^{5+} and V^{4+} was faster than C^{4+}, which led to increase the outer layer as compared to inner layer, whereas growth of region 3reducedthe volume of region 2, being the major loss of WC phase. Samples sintered for 2 h showed negligible growth of the innermost region, as well as minimum thickness of the outer layer (Fig. 6). As the sintering time increased, the volume fraction of WC decreased in most of the samples due to decomposition of WC. It was observed that when holding time increased to 8 h, the volume fraction of WC along with η phase decreased and samples become weaker due to localized non-uniformity in the constituents.

3.4 Hardness and fracture toughness

Hardness and fracture toughness are inversely proportional to each other. Obtaining high hardness with good fracture toughness, through conventional sintering at low temperature is always desirable. Fig. 8 shows the micro-hardness of the WC-20Co samples sintered at 1100 °C. The present study evolved with a unique result of getting hardness in the range of 1687 (HV)and fracture toughness of 13.5 $MPa.m^{-3/2}$ with 20 wt% Co, which is much higher than the values reported earlier with this composition sintered at 1100 °C through conventional liquid phase sintering[6,11,14,41]. Only two samples, P4 and P5 with 7.5 and 10 wt. % VC, respectively, sintered for 2 h, showed maximum value and all other samples exhibit poor hardness in the range of 223 (HV). Use of nanopowder as raw material was intended to lower the sintering temperature. Fig. 8 represents the variation of hardness with respect to sintering time and content of VC. Volume fraction of hard phase (WC) was higher in the samples sintered for 2 h, thereafter it decreased with increased holding time (Table 2 and Fig. 4). In contrast, formation of Co_6W_6C at 1100 °C[4,11], observed an appreciable increase in volume fraction with increase in holding time of 6 h, after that it decreased. Fig. 8 and Fig. 9 depict a good combination of hardness and toughness depending upon the holding time and wt. % of VC for P4 sample. Other samples did not show crack at the indentation due to partial sintering, poor densification and higher porosity has demonstrated good fracture toughness since pores/voids act as crack arrestors[6].The role of high VC content seemed to be more effective in controlling the formation of Co_6W_6C when the sintering time was increased beyond 4 h. It was evident

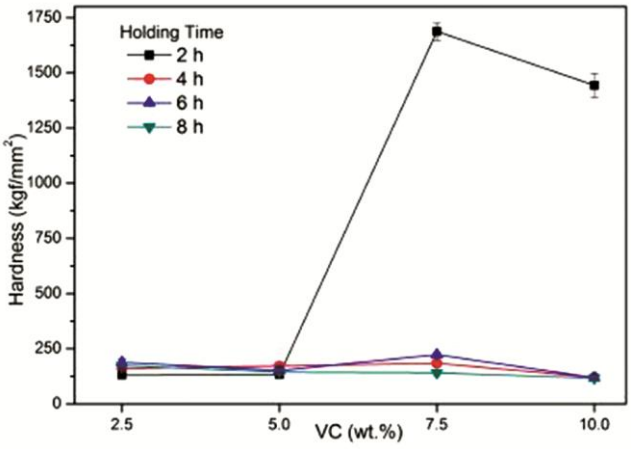

Fig. 8 — Microhardness of the all the sintered samples at 1100 °C for different holding time.

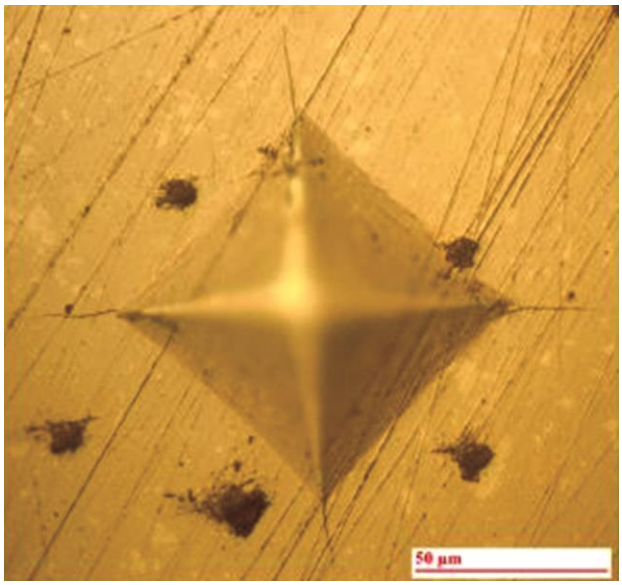

Fig. 9 — Indentation on sintered sample P4 for 2 h holding time.

from Fig. 4 that volume fraction of Co_6W_6C and WC was totally reversed and depends on the wt. % of VC. In all the samples, the high hardness was observed when WC and Co_6W_6C phases are approximately in the ratio of 2:1 without free carbon.

4 Conclusions

Longer holding time with higher content of VC decreases the density of most of the samples. High wt. % of VC acts as a hardener for 2 h of isothermal holding. Increased sintering duration, the thickness of brittle outer layer along with porosity of the samples is increased. In samples P4 (7.5 wt. % of VC) and P5 (10 wt. % of VC) with holding time 2 h, the ratio of volume fraction of WC and Co_6W_6C is 2:1. The

hardness value of 1687 (HV) and indentation fracture toughness of 13.5 $MPam^{-3/2}$ is observed in sample P4. The volume fraction of different crystalline phases depends on VC content and isothermal holding time for sintering. Material with high hardness and good fracture toughness can be prepared by selecting proper process parameters with initial constituents at lower sintering temperature *i.e*., 1100 °C for tool application.

Acknowledgement

The authors would like to thank Technical Education Quality Improvement Program (TEQIP-II) for financial support.

References

1 Wang X, Fang Z Z & Sohn H Y, *Int J Ref Met Hard Mater*, 26 (2008) 232.
2 Su W, Sun Y, Feng J, Liu J & Ruan J, *Int J Ref Met Hard Mater*, 48 (2015) 369.
3 Fang Z, Maheshwari P, Wang X & Sohn H Y, *Int J Ref Met Hard Mater*, 23 (2005) 249.
4 Eso O, Fang Z Z & Griffo A, *Int J Ref Met Hard Mater*, 25 (2007) 286.
5 Shi X L, Shao G Q, Duan X L, Xiong Z & Yang H, *Mat Char*, 57 (2006) 358.
6 Al-Aqeeli N, Mohammad K, Laoui T & Saheb N, *Mater Man Pro*, 30 (2015) 327
7 Morton C W, Wills D J & Stjernberg K, *Int J Ref Met Hard Mater*, 23 (2005) 287.
8 Poetschke J, Richter V, Gestrich T & Michaelis A, *Int J Ref Met Hard Mater*, 43 (2014) 309.
9 Sun X, Wang Y& Li DY, *Wear*, 301 (2013) 406.
10 Chen H, Yang Q & Yang J *et al*., *J Alloys Compd*, 714 (2017) 245.
11 Upadhyaya G S, *Cemented Tungsten Carbides: Production, Properties and Testing*, New Jersey, Noyes Publications, (1998).
12 Kurlov A S, Gusev A I & Rempel A A, *Int J Ref Met Hard Mater*, 29 (2011) 221.
13 Tao L, Quingfa L, Fuh J Y H & Wu C C, *Mater Sci Eng A*, 430 (2006) 113.
14 Fang Z Z, Wang X, Ryu T, Hwang K S & Sohn H Y, *Int J Ref Met Hard Mater*, 27 (2009) 288.
15 Fang Z Z, Correlation of Transverse Rupture Strength of WC-Co with Hardness, *Int J Refrect Met H*, 23 (2005) 119.
16 Kumar A, Singh K & Pandey O P, *Ceram Int*, 37 (2011) 1415.
17 Bonache V, Salvador M D , Busquets D , Burguete P & Martinez E, et al., *Int J Ref Met Hard Mater*, 29 (2011) 78.
18 Kurlov A S & Gusev A I, **Hard metals WC–Co Based on Nanocrystalline Powders of Tungsten Carbide WC**, Tungsten Carbide: Springer Series in Material Science, (2013) ISBN: 978-3-319-00524-9**.**
19 Xie H, Liu Y, Ye J, Li M & Zhu Y H., et al, *Int J Ref Met Hard Mater*, 47(2014)145.
20 Aqeeli NA, Mohammad K, Laoui T & Saheb N, *Ceram Int*, 40 (2014) 11759.
21 Gu L, Huang J & Xie C, *Int J Ref Met Hard Mater*, 42 (2014) 228.
22 Okamoto S, Nakazono Y, Otsuka K, Shimoitani Y & Takada, *Mater Charact*, 55 (2005) 281.
23 Shaw L L, *Mater Man Pro*, 16 (2001) 405.
24 Cho K C, Woodman R K, Klotz B R, Dowding R J, *Mater Man Pro*, 190 (2004) 619.
25 Gurwell W E, *Mater Man Pro*, 9 (1994) 1115.
26 Yoo S H, Sudarshan T S, Sethuram K, Subhash G & Dowding R J, *Mater Man Pro*, 42 (1999) 181.
27 Furushima R, Katou K, Shimojima K, Hosokawa H, Matsumoto A, *Int J Ref Met Hard Mater*, 50 (2015) 16.
28 Carroll D F, *Int J Ref Met Hard Mater*, 17 (1999) 123.
29 Lee H R, Kim D J, Hwang N M & Kim D Y, *J Am Cer Soc*, 86 (2003) 152.
30 Cha S I, Hong S H, Ha G H & Kim B K, *Scr Materialia*, 44 (2001) 1535.
31 Sugiyama I, Mizumukai Y, Taniuchi T, Okada K & Shirase F et al, *Scr Mater*, 69 (2013) 473.
32 Lay S, Thibault S H & Loubrado M, Inter Sci, 12 (2004) 187.
33 Jaroenworaluck A, Yamamoto T, Ikuhara Y, Sakuma T & Taniuchi T et al, *J Mater Res*, 13 (1998) 2450.
34 Seo O, Kang S & Lavernia E J, *Mater Tran*, 44 (2003) 2339.
35 Mahmoodan M, Aliakbarzadeh H & Shahri F, *J Nano Sci Eng*, 3 (2013) 35.
36 Jia K, Fischer T E & Gallois B, *Nano Str Mat*, 10 (1998) 875.
37 Espinosa L, Bonache V & Salvador M D, *Wear*, 1 (2011) 62.
38 Srivatsan T S, Woods R, Petraroli M & Sudarshan T S, *Pow Tech*, 122 (2002) 54.
39 X Q Ou, Song M, Shen T T, Xiao D H & He Y H, *Int J Ref Met Hard Mater*, 29 (2011) 260.
40 Kumar D & Singh K, *Mater Sci Eng A*, 663 (2016) 21.
41 Kumar D, Singh K, *Mater Man Pro*, 30 (2015) 1329.
42 Carneim R D & Messing G L, *Pow Tech*, 115 (2001) 131.
43 Soleimanpour A M, Abachi P, Simchi A, *Int J Ref Met Hard Mater*, 31 (2012) 141.
44 Cho K C, Woodman R H, Klotz B R & Dowding R J, *Mat Manu Pro*, 19 (2004) 619.
45 Mahmoodan M, Aliakbarzadeh H & Shahri F, *J Nano Sci Eng*, 3 (2013) 35.
46 Kumar A, Singh K, Pandey O P, *Cera Int*, 37 (2011) 1415.
47 Xiong Z, Shao G, Shi X, Duan X, Yan L, *Int J Ref Met Hard Mater*, 26 (2008) 242.
48 Cullity B D, **Elements of X-Ray Diffraction**, 2nd edition, Addison Wesley Publication Company, (1978), ISBN: 0201011743, 9780201011746**.**
49 Kim H C, Oh DY, Shon I J, *Int J Ref Met Hard Mater*, 22 (2004) 197.
50 Anstis G R, Chantikul P, Lawn B R, Marshall D B, *J Am Ceram Soc*, 64 (1981) 533.
51 Sun Z, Ahuja R & Lowther J E, *Sol St Comm*, 150 (2010) 697.
52 Morton C W, Wills D J & Stjernberg K, *Int J Ref Met Hard Mater*, 23 (2005) 287.
53 Cho S A, Hernandez A, Ochoa A & Olivares J L, *Int J Ref Met Hard Mater*, 15 (1997) 205.
54 Sert A & Cilik O N, *Mat Char*, 150 (2019) 1.
55 Cilik O N, Sert A, Gasan H & Ulutan M, *Int J Adv Man Tech*, 95 (2018) 2989.
56 Sabzi M, Mousavi A S H, Ghobeiti-Hasab M, Fatemi-Mehr M, *J Alloys Compd*, 766 (2018) 672.
57 Sabji M, Mousavi S H, Asadin M, *Int J Appl Ceram Technol*, 15 (2018) 1350.